Supporting Information

Schwartzman et al. 10.1073/pnas.1418580112

SI Materials and Methods

General Procedures. Bacterial strains and plasmids used in this work are listed in Table S2. All *Vibrio fischeri* mutant strains are derived from isolate ES114 (1, 2). *V. fischeri* and *Vibrio harveyi* cells were grown at 28 °C, with shaking at 225 rpm, unless otherwise noted. In *V. fischeri* culture experiments, 5 μg erythromycin (Em)·mL^{-1} or 100 μg kanamycin (Kn)·mL^{-1} were added where indicated. *V. fischeri* cultures were grown in high-osmolarity seawater tryptone medium (SWTO) (3), Luria–Bertani salt medium (LBS) (4), or minimal salts medium (MSM). *Escherichia coli* was cultured at 37 °C with shaking at 250 rpm in Luria–Bertani medium (LB) (5) or M9 minimal medium (6). Where indicated, 50 mM Pipes buffer (pH 7.5), 150 μg Em·mL^{-1}, or 50 μg Kn·mL^{-1} was added to *E. coli* cultures.

Adult squid, collected at Oahu, Hawaii, were maintained in the laboratory in circulating 35-ppt Instant Ocean (Aquarium Systems), on a 12-h/12-h light/dark cycle. Squid were colonized and raised as described previously (7, 8), with the following modifications: Animals were exposed to ∼5,000 colony-forming units (cfu)/mL of the indicated *V. fischeri* strains in filter-sterilized Instant Ocean for 16 h, euthanized, and frozen at −80 °C. Animals were anesthetized for 5 min in seawater containing 2% (vol/vol) ethanol for collection of blood and tissue samples. The mature light-organ developmental state was distinguished in living animals by (*i*) a mantle length of >10 mm and (*ii*) a behavioral transition of the animals to a pattern of nocturnal activity. All animal experiments meet the regulatory standards established for invertebrates by the University of Wisconsin–Madison.

***Es*Chit1 Antibody Design and Validation.** A polyclonal rabbit antibody against the squid chitotriosidase 1 (*Es*Chit1; Genscript) was generated to the synthetic peptide sequence (CYPGSRGSPAVDKKN) that is predicted to be located at an internal, but surface-exposed, portion of the protein (Fig. S5) and that lacked any significant match to other sequences in the squid databases. To determine the specificity of the anti-*Es*Chit1antibody (α-*Es*Chit1), we performed a Western blot analysis, as previously described (9). The protocol was modified so that proteins were transferred to a 0.2-μm nitrocellulose membrane and blocked overnight in a solution containing 4% (wt/vol) milk in 0.1% Tween-20 in Tris-buffered saline (TBS) (20 mM Tris with 0.5 M NaCl, pH 7.4) at 4 °C. After blocking, the membranes were incubated for 3 h at room temperature in 4% milk in 0.1% Tween-20, with either a 1:250 dilution of α-*Es*Chit1 or purified rabbit IgG at the same concentration as a negative control. Secondary antibody and detection of antibody hybridization were performed as described elsewhere (9). This antibody was highly specific relative to an Ig control by Western blot against light-organ central-core tissues, at a concentration of 1:250 (Fig. 2*B*), and was also used for immunochemistry at this concentration (10, 11).

Immunocytochemistry, Fluorescence Microscopy, and Hemocyte Characterization. Fluorochromes were obtained from Life Technologies, and all other chemicals were purchased from Sigma-Aldrich, except where indicated. Immunocytochemistry (ICC) and processing of squid tissues were performed as described previously (10), with minor modifications, described below. All samples were mounted in Vectashield (Vector Laboratories) before observation by confocal microscopy. A Zeiss 510 laser-scanning confocal microscope with AxioImager software (Carl Zeiss Instruments) was used to image samples, unless otherwise noted.

Collection of adult central-core tissue, juvenile light organs, and hemocytes. Central-core tissue was collected from squid >18 mm in mantle length. The light organ was exposed by ventrally dissecting the mantle and removing the funnel. The central cores are located bilaterally on the light organ, in a pocket defined by layers of ink sac and reflector (Fig. 1*A*). The lobes of the organ are surrounded by vitreous lens tissue. To expose the central-core tissue, the lens was dissected just above where the ink sac and reflective tissue fold around the central core, located on the outer edge of the light organ. Weak connective tissue joins the tissue folds between which the central core is located. If this tissue could be removed to fully unfold the reflector and ink sac, then the central core was removed immediately and incubated in a fixative containing 4% (vol/vol) paraformaldehyde (PFA) in mPBS (50 mM sodium phosphate, pH 7.4, 0.4 M NaCl) for 16 h at 4 °C to stabilize the tissues. If the central-core tissue could not be removed without compromising its structural integrity, then the whole light organ was removed from the squid's mantle cavity by cutting the connective tissues underneath the organ, as well as the gut and ligaments attaching it from above, and placing the organ in 4% PFA in mPBS for 5 min, before removal of central-core tissues. Fixed samples were rinsed three times for 10 min in mPBS and then permeabilized 24 h in 1% Triton-X100 in mPBS. Immature light organs were collected as described elsewhere, with minor modifications (11). The light-organ ink sac was gently punctured during dissection to permit drainage of ink and better visualization of deep crypt structures. Hemocyte isolation was performed as described previously (12). Briefly, 15-μL samples of squid hemolymph, extracted from the cephalic vessel, were applied to glass coverslips, and hemocytes were allowed to adhere for 30 min. Following this step, the slides were rinsed three times in Squid Ringer's buffer [530 mM NaCl, 10 mM KCl, 25 mM $MgCl_2$, 10 mM $CaCl_2$, and 10 mM Hepes buffer, pH 7.5 (13)] to remove nonadherent cells, and the samples were fixed for 30 min in 4% PFA in mPBS and permeabilized for 30 min in 1% Triton-X100 in mPBS (mPBST).

Detection of chitin and hemocytes by fluorescent probes. Immature light organs, or central-core tissue, were incubated for 7 d in a 1:250 dilution of TRITC-conjugated chitin-binding protein (CBP) (New England Biolabs) in mPBST (12). To counterstain, tissues were incubated 4 d in a 1:40 dilution of FITC-conjugated DNase-I to visualize hemocytes by their enrichment in globular actin (14) and 25 μg/mL Alexa-633 phalloidin in for 2 d to visualize the actin cytoskeleton. Hemocytes were incubated at room temperature for 3 h with 1:250 FITC-conjugated CBP in mPBST, rinsed, and counterstained with 1:40 rhodamine phalloidin in mPBST overnight at 4 °C to visualize the actin cytoskeleton. A 1:500 dilution of TOTO-3 iodide was added for 10 min at room temperature to visualize nuclear DNA.

Detection of predicted squid chitinases by immunocytochemistry. Permeabilized central-core tissues were incubated at 4 °C with mPBST block (0.5% goat serum and 1% BSA in mPBST) overnight and then for 7 d with a 1:500 dilution of α-*Es*Chit1 primary antibody, or the same concentration of purified rabbit IgG as a negative control, in mPBST block. To visualize antibody binding, samples were incubated overnight in a 1:40 dilution of TRITC-conjugated goat anti-rabbit/chicken secondary antibody. Tissues were counterstained in mPBST for 4 d in a 1:40 dilution of FITC-conjugated DNase-I and overnight with 25 μg Alexa-633 phalloidin per milliliter. Hemocytes were incubated at room temperature in mPBST block for 1 h, then in primary antibody in mPBST block for 3 h, and finally in a 1:40 dilution of FITC-conjugated goat anti-rabbit in mPBST blocking solution

for 45 min. Samples were counterstained overnight at 4 °C with a 1:40 dilution of rhodamine phalloidin in mPBST and for 10 min at room temperature with a 1:500 dilution of TOTO-3 iodide to visualize nuclear DNA.

Enumeration of hemocytes in immature light organs and visualization of mature central-core tissue. To enumerate hemocytes present in immature light organs, samples stained with FITC-DNase-I and rhodamine phalloidin, as described above, were visualized by confocal microscopy. Hemocytes, defined as DNase-I positive cells, were enumerated in a region of the light organ extending from the midaxis line to the ciliated epithelial field. Hemocytes present in the anterior and posterior appendages (structures characteristic of the immature light organ and not present in the fully mature structure) were not enumerated in this analysis. To visualize fluorescently labeled structure in central-core tissue, we located a field of view where the tissue surface was relatively uniform (i.e., the surface tissue had not been disrupted by dissection). Although the boundaries of crypts could not be definitively identified with the fluorescent probes used, we analyzed fields of view where phalloidin, which stains the actin cytoskeleton, formed a honeycomb-like structure, reminiscent of the finger-like projections of the mature light-organ crypt (Fig. 1*A*).

Collection and characterization of expelled crypt contents. To collect crypt contents, anesthetized squid were exposed to a light cue to induce venting behavior, as described previously (15). Acidic compartments of these cells were labeled by staining for 30 min with a 1:500 diution of Lysotracker Red in Squid Ringer's buffer and visualized by epifluorescence microscopy. To assess nuclear-membrane integrity, cells were stained for 5 min with a 1:10,000 dilution of acridine orange and visualized by confocal microscopy. For analysis of chitin and immunocytochemistry, the expelled crypt contents were collected with a negative-pressure pipette and placed directly in 4% PFA in mPBS for 4 h. A 20-μL sample of whole hemolymph was also collected as a control to compare cell morphology and staining patterns. Samples were suspended in Histogel matrix (Richard-Allen Scientific; HG-4000-012) and then embedded in paraffin and cut into 5-μm sections. The sections were deparaffinized and stained with hematoxylin and eosin to identify hemocytes (16). Embedding, sectioning, and staining were performed by the Histology Core Facility in the Surgery Department at the University of Wisconsin–Madison School of Medicine and Public Health. Unstained sections were also processed for fluorescence microscopy and immunocytochemistry, using a previously developed protocol (9). The same concentrations of fluorochromes and antibodies were used as described for staining central-core tissue, light organs, and hemocytes.

Morphological changes of hemocytes exposed to crypt contents. To characterize acidic compartments in hemolymph-derived hemocytes upon exposure to the light-organ crypt contents, hemocytes were collected, incubated with Lysotracker Red as described above, and then centrifuged at 15,800 × *g* for 10 min at 4 °C in a tabletop centrifuge to remove excess dye. The cells were resuspended in Squid Ringer's buffer adjusted to either pH 7.5 or pH 5.5 [the nocturnal crypt pH (9)]. Fresh crypt contents were collected from the same animal and placed on ice. When the hemolymph-derived hemocytes had been labeled, 5 μL of fresh crypt contents was added to 20 μL of labeled hemocytes in either pH 7.5 or pH 5.5 buffer. The remaining crypt contents were heated to 95 °C for 10 min, to inactivate heat-labile crypt-contents components. Five microliters of heat-exposed crypt contents were added to 20 μL of Lysotracker-Red–labeled cells in pH 7.5 buffer. Samples were incubated for 2 h and then visualized using a Zeiss Axio Imager M2 epifluorescence microscope. To ensure that morphological irregularities were not a result of experimental manipulations, a control population of hemocytes was collected and processed in the same manner as that of the experimental samples, except that the hemocytes were not exposed to crypt contents.

RNA Extraction, Sequence Characterization, and Quantitative RT-PCR. The full-length *eschit1* transcript was obtained by RACE amplification, as described previously (9) (Fig. S5). The sequence was deposited in GenBank (accession no. KM592978). cNA synthesized from juvenile light organ total RNA was used as the template. The sample collection and transcriptional analysis were performed as described previously (9). Three-day-old and 4-wk-old light organs collected at 2 h, 10 h, and 22 h postdawn (hpd) were dissected in RNAlater (either $n = 4$ replicates of 20 juvenile light organs per replicate or $n = 4$ replicates of 5 adult light organs per replicate). To correct for the presence of bacterial symbiont RNA in the samples, amounts of total RNA added to the cDNA synthesis reactions were scaled, as follows: 2 hpd, 1×; 10 hpd, 1.1×; 22 hpd, 1.2×. Primer-set efficiencies were between 95% and 105% as determined by standard curves, using 10-fold dilutions of template. Primers are listed in Table S3. A 60 °C annealing temperature was used for all primer pairs. Candidate gene expression was normalized using the geometric mean of 40S ribosomal RNA and serine hydroxymethyltransferase (serine HMT) expression values. The distribution of the data was measured by Shapiro's test (all data fitted a normal distribution), and a two-way ANOVA with post hoc Bonferroni comparison was used to compare gene expression among time points and between colonization states.

Quantitative RT-PCR procedures were conducted in accordance with the MIQE guidelines (17) for sample collection, RNA isolation, cDNA synthesis, quantitative RT-PCR amplification, normalization of experimental gene expression using reference genes, and data analysis. Primers were designed by OligoAnalyzer software (Integrated DNA Technologies) (Table S2).

Molecular Genetics. All plasmids were constructed and introduced into *V. fischeri* with standard molecular techniques (18). To construct a vector for *in trans* complementation of the *nagB* gene deletion, a segment of DNA corresponding to 500 bp upstream and 100 bp downstream of the annotated *nagB* coding sequence was amplified using primers with unique restriction sites engineered at the 5′ end and cloned into the *V. fischeri* Tn*7*-site integration plasmid, pEVS107 (18) (Table S2). The plasmid was introduced into the appropriate *V. fischeri* strain by conjugative transfer and integrated into the Tn*7* locus with the help of the pUXBF13 plasmid, as previously described (18–20) (Table S2).

Growth-Yield Measurement. To assess growth on a sole source of carbon, strains were cultivated for 24 h in MSM (21), modified as described previously (22). The medium was buffered at pH 7.5 with 50 mM Pipes and contained either 5 mM di-*N*-acetyl chitobiose (Cayman Chemicals) or 10 mM *N*-acetylglucosamine, glucosamine, or glucose. Strains were first grown as LBS cultures and then subcultured 1:100 into 0.2% casamino acids in MSM until they reached an optical density (600 nm, 1 cm path length, OD_{600}) of 0.40 ± 0.05 absorbance units. These cultures were used to inoculate (at a dilution of 1:100) MSM supplemented with a single carbon source. Optical density was determined after 36 h of growth.

Acid Tolerance Assays. Induction of acid tolerance in *V. fischeri* was assessed using a modified version of the acid-killing assays developed for *Vibrio cholerae* (23). To measure induction of acid tolerance in cultured cells, 30-mL SWTO cultures of *V. fischeri* were grown in 125-mL flasks with shaking to an OD_{600} of 0.4 ± 0.05. Cells were harvested by centrifugation for 6 min at 5,000 × *g*. To measure the potential for cells to adapt to a sublethal amount of organic-acid stress, 90% of the cells were resuspended in 0.5 mL SWTO (pH 5.5) containing 50 mM Pipes and 0.075× organic

acids (1× organic acids = 74 mM propionic acid, 174 mM acetic acid, and 50 mM butyric acid). The remaining 10% of the cells were resuspended in 0.5 mL SWTO (pH 7.5) containing 50 mM Pipes without organic acids. Cell suspensions were incubated for 1 h at 28 °C with shaking, before centrifugation, and pellet resuspension in 0.5 mL SWTO (pH 4.75) containing 0.1× organic acids and 50 mM Pipes. Aliquots of cells (20 μL) were removed at 10-min intervals and serially diluted, and 10 μL of each dilution was spotted onto LBS agar plates for colony enumeration. Percentage survival at time T_n was calculated by (cfu/mL)T_n − (cfu/mL)T_0 × 100. To assay for induction of acid tolerance by catabolism of COS, cells were grown in 30 mL of 20 mM COS in SWTO (pH 7.5) with and without an additional 50-mM Pipes buffer, pelleted, and resuspended directly in SWTO (pH 4.75) containing 50 mM Pipes and 0.1× organic acids.

To assay the induction of acid tolerance in symbiotic cells of *V. fischeri*, symbiont-containing tissues (from mature squid with mantle length >15 mm), whole light organs (from squid with 10–15 mm mantle length) or batches of 50 whole light organs (from juvenile squid with <10 mm mantle length) were gently homogenized to release bacterial cells. Symbiont-containing supernatant from the light-organ homogenate was pelleted by centrifugation, and survival was compared between populations resuspended directly in lethal SWTO (pH 4.75) containing 50 mM Pipes and 0.1× organic acids or following a 1-h incubation under the inducing condition of SWTO (pH 5.5) containing 50 mM Pipes and 0.075× organic acids.

Acetate and Glucose Detection. Samples of *V. fischeri*, *V. harveyi*, or *E. coli* culture supernatant were assayed for acetate production and glucose consumption: Cells were grown in 3 mL LBS (*Vibrio* spp.) or LB (*E. coli*) broth to OD_{600} of 0.5 ± 0.05, and 0.25 mL of these cultures was pelleted, rinsed, and resuspended in 3 mL of MSM (for *Vibrio* spp.) (21) or M9 (for *E. coli*) (24) containing either 5 mM GlcNAc or 5 mM glucose. MSM and M9 are both minimal media, containing similar profiles of minerals, at different compositions. These media have been previously optimized for the growth of marine (MSM) or terrestrial (M9) microbes. Cultures were grown with shaking in 18-mm test tubes at 225 rpm for 2 h. To determine the level of acetate accumulation in the minimal medium supernatant, 100-μL aliquots of bacterial cultures at an OD_{600} of 0.5 ± 0.05 were centrifuged for 15 min at 13,000 × *g* and 4 °C to remove cells. The cell-free supernatant was stored at −20 °C until assayed. A coupled-enzyme assay (Sigma-Aldrich; no. MAK086) was used to detect acetate, following the manufacturer's protocol. Absorbance at 420 nm was monitored to detect the accumulation of the colorimetric substrate with a TECAN plate reader and Magellan automation software (Tecan Group). The concentration of acetate in the culture supernatant was calculated based on a linear regression of measurements for acetate standards of known concentration (R^2 = 0.93, over a range of 0–300 μM). Where necessary, samples were diluted to fall within the detection limits of the assay. The amount of acetate per cell was divided by the OD_{600} to normalize between conditions. Glucose was detected by a glucose-oxidase coupled-enzyme assay (Sigma-Aldrich; no. GAGO20), following the manufacturer's protocol. Absorbance at 600 nm was monitored to detect *o*-dianisidine, the colorimetric product, proportional to the original glucose concentration. The concentration of glucose in the culture supernatant was calculated by a comparison with a calibration curve generated from standards of known glucose concentration (R^2 = 0.99, over a range of 0–500 μM glucose). Samples were diluted as necessary to fall within the linear range of glucose concentration detected by the assay, as defined by the calibration curve.

Hemolymph Titration. To determine the buffering capacity of hemolymph, 100-μL samples of cell-free hemolymph were first diluted 1:10 in deionized water and then titrated with 0.1 M HCl. pH measurements were made using an Orion PerpHect LogR meter and a Silver/Silver Chloride reference electrode (ThermoFisher Scientific).

SI Calculations

Calculations in Support of COS Delivery by Hemocytes. Assumptions and measured quantities:

i) It takes ∼7.5 mM acetate to acidify hemolymph to pH 5.5 (Fig. S4*E*).
ii) The theoretical yield of acetate is three molecules of acetate per molecule of GlcNAc.
iii) Because COS are made of GlcNAc monomers, these calculations are done assuming GlcNAc is the form of COS.
iv) The molecular weight of GlcNAc is 221 g/mol.
v) The crypt contents are ∼20 μL and contain 10^3–10^4 hemocytes (15).
vi) The density of GlcNAc is 1.5 g/cm^3.
vii) The hemolymph is approximately pH 7 (9).

About How Much COS Would It Take to Acidify the Light Organ?

i) It takes ∼7.5 mM acetate to acidify hemolymph from pH 7 to pH 5.5 (Fig. S4*E*).
Assume that the volume acidified is ∼20 μL hemolymph (vented volume) (15) and that acetate is the major acidic component:

$$7.5\times10^{-3}\ \text{mol acetate/L} * 20\times10^{-6}\text{L} = 1.5\times10^{-7}\ \text{mol acetate}$$

$$1.5\times10^{-7}\ \text{mol acetate} * 1\ \text{mol COS}/3\ \text{mol acetate} = \sim 5\times10^{-8}\ \text{mol COS/light organ}$$

$$5\times10^{-8}\ \text{mol COS/light organ} * 221\ \text{g/mol} = \sim 11\ \mu\text{g COS/light organ.}$$

Although the epithelial cells could take up acetate (pK_a 4.76), 75% of the acetate will carry a negative charge when the nocturnal crypt pH is 5.5, suggesting that unless acetate uptake is an active process, the amount of protonated acetate lost from the crypt lumen by epithelial absorption will be small.

ii) COS cannot be present at concentrations much greater than 2.5 mM at one time, because the cocolonization of *ΔnagB* and wild type is not biased toward wild type (Fig. S3 *D* and *E*).
A total of 2.5 mM COS is equivalent to 11 μg in a 20-μL crypt volume.

About How Many Hemocytes Would It Take to Deliver This Amount of COS? If each hemocyte releases eight 1-μm diameter spherical granules of COS,

$$\text{The volume of the chitin granule} = \sim 5\times10^{-10}\ \text{cm}^3.$$

$$1.5\ \text{g/cm}^3 * 5\times10^{-10}\ \text{cm}^3 = 7.5\times10^{-10}\ \text{g/granule} * 8\ \text{granules/cell} = \sim 6\times10^{-3}\mu\text{g GlcNAc per cell.}$$

This means that the calculated 11 μg COS could be delivered by ∼2,000 hemocytes.

Previous quantification of hemocytes in crypt contents was estimated at 10^3–10^4 hemocytes per light-organ crypt (15).

1. Boettcher KJ, Ruby EG (1990) Depressed light emission by symbiotic *Vibrio fischeri* of the sepiolid squid *Euprymna scolopes*. *J Bacteriol* 172(7):3701–3706.
2. Mandel MJ, Stabb EV, Ruby EG (2008) Comparative genomics-based investigation of resequencing targets in *Vibrio fischeri*: Focus on point miscalls and artefactual expansions. *BMC Genomics* 9:138.
3. Stabb EV, Butler MS, Adin DM (2004) Correlation between osmolarity and luminescence of symbiotic *Vibrio fischeri* strain ES114. *J Bacteriol* 186(9):2906–2908.
4. Graf J, Dunlap PV, Ruby EG (1994) Effect of transposon-induced motility mutations on colonization of the host light organ by *Vibrio fischeri*. *J Bacteriol* 176(22):6986–6991.
5. Sambrook J, Fritsch EF, Maniatis T (1989) *Molecular Cloning* (Cold Spring Harbor Lab Press, Cold Spring Harbor, NY).
6. Miller JH (1972) *Experiments in Molecular Genetics* (Cold Spring Harbor Lab Press, Cold Spring Harbor, NY).
7. Lynn MN, Mark JM (2012) Colonization of *Euprymna scolopes* squid by *Vibrio fischeri*. *J Vis Exp* 61:e3758.
8. Koch EJ, Miyashiro T, McFall-Ngai MJ, Ruby EG (2014) Features governing symbiont persistence in the squid-vibrio association. *Mol Ecol* 23(6):1624–1634.
9. Kremer N, et al. (2014) The dual nature of haemocyanin in the establishment and persistence of the squid-vibrio symbiosis. *Proc Biol Sci* 281(1785):20140504.
10. Troll JV, et al. (2009) Peptidoglycan induces loss of a nuclear peptidoglycan recognition protein during host tissue development in a beneficial animal-bacterial symbiosis. *Cell Microbiol* 11(7):1114–1127.
11. Kremer N, et al. (2013) Initial symbiont contact orchestrates host-organ-wide transcriptional changes that prime tissue colonization. *Cell Host Microbe* 14(2):183–194.
12. Heath-Heckman EA, McFall-Ngai MJ (2011) The occurrence of chitin in the hemocytes of invertebrates. *Zoology* 114(4):191–198.
13. Nyholm SV, Stewart JJ, Ruby EG, McFall-Ngai MJ (2009) Recognition between symbiotic *Vibrio fischeri* and the haemocytes of *Euprymna scolopes*. *Environ Microbiol* 11(2):483–493.
14. Altura MA, et al. (2013) The first engagement of partners in the *Euprymna scolopes-Vibrio fischeri* symbiosis is a two-step process initiated by a few environmental symbiont cells. *Environ Microbiol* 15(11):2937–2950.
15. Nyholm SV, McFall-Ngai MJ (1998) Sampling the light-organ microenvironment of *Euprymna scolopes*: Description of a population of host cells in association with the bacterial symbiont *Vibrio fischeri*. *Biol Bull* 195(2):89–97.
16. Sheehan DC, Hrapchak BB (1980) *Theory and Practice of Histotechnology* (Mosby, St Louis).
17. Bustin SA, et al. (2009) The MIQE guidelines: Minimum information for publication of quantitative real-time PCR experiments. *Clin Chem* 55(4):611–622.
18. McCann J, Stabb EV, Millikan DS, Ruby EG (2003) Population dynamics of *Vibrio fischeri* during infection of *Euprymna scolopes*. *Appl Environ Microbiol* 69(10):5928–5934.
19. Bao Y, Lies DP, Fu H, Roberts GP (1991) An improved Tn7-based system for the single-copy insertion of cloned genes into chromosomes of gram-negative bacteria. *Gene* 109(1):167–168.
20. Stabb EV, Ruby EG (2002) RP4-based plasmids for conjugation between *Escherichia coli* and members of the Vibrionaceae. *Methods Enzymol* 358:413–426.
21. Adin DM, Visick KL, Stabb EV (2008) Identification of a cellobiose utilization gene cluster with cryptic β-galactosidase activity in *Vibrio fischeri*. *Appl Environ Microbiol* 74(13):4059–4069.
22. Miyashiro T, et al. (2011) The *N*-acetyl-D-glucosamine repressor NagC of *Vibrio fischeri* facilitates colonization of *Euprymna scolopes*. *Mol Microbiol* 82(4):894–903.
23. Merrell DS, Camilli A (1999) The *cadA* gene of *Vibrio cholerae* is induced during infection and plays a role in acid tolerance. *Mol Microbiol* 34(4):836–849.
24. Anonymous (2010) M9 minimal medium (standard). *Cold Spring Harb Protoc* 2010(8): pdb.rec12295.

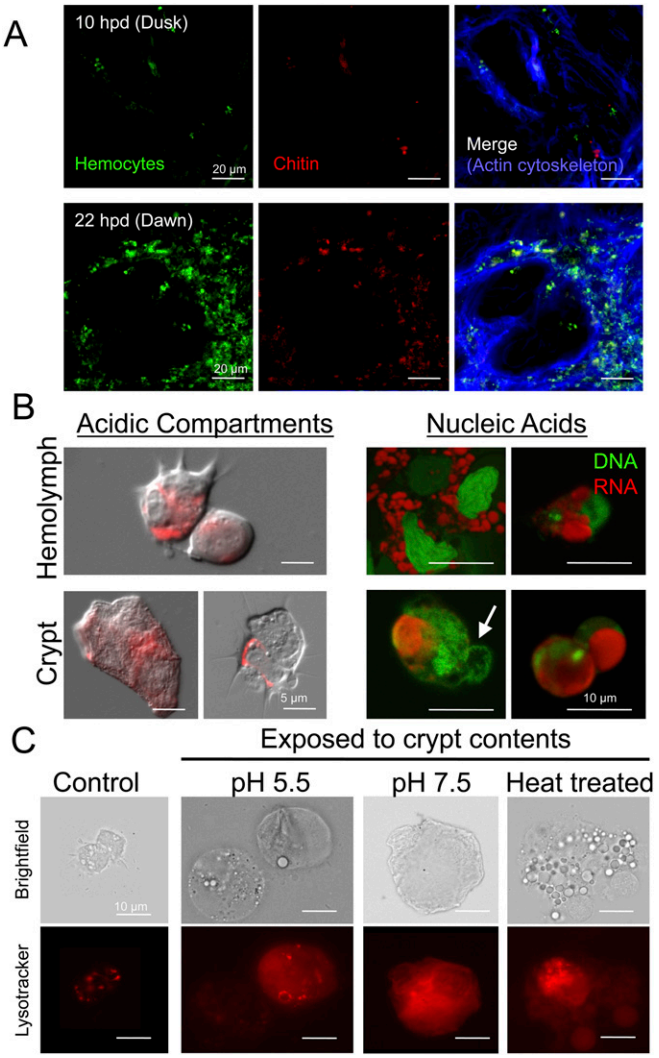

Fig. S1. Presence of chitin and hemocytes in light-organ tissue and morphological changes of hemocytes exposed to the light-organ crypt environment. (*A*) Confocal micrographs, showing colocalization of fluorescently labeled hemocyte-specific marker DNase-I (green, FITC label, binds globular actin) and chitin-specific chitin-binding protein (red, TRITC label, binds particulate chitin). Actin-rich extracellular matrix was detected with Alexa 633 phalloidin (blue). Tissue was sampled at dusk (*Top*, 10 h postdawn, hpd) and before dawn (*Bottom*, 22 hpd). (*B*, *Left*) Morphology of hemocytes derived from the squid hemolymph (*Top*) and the light-organ crypt (*Bottom*). Images are merged differential interference contrast and fluorescent micrographs. Acidic compartments within cells were labeled with Lysotracker Red. (*Right*) DNA (green) and RNA (red) were labeled with acridine orange. Arrow indicates irregular nuclear morphology. (*C*) Morphological changes are induced in hemocytes upon exposure to crypt contents. Hemolymph (containing hemocytes) and crypt contents were collected from a single animal at 22 hpd. (*Left*) The acidic vesicles of these hemocytes were labeled with Lysotracker Red. The labeled cells were then exposed to 25% crypt contents in pH 5.5, the nocturnal pH of the crypt (1), in Squid Ringers buffer, and monitored over time. (*Center Left*, *Center Right*, and *Right*) Blebbing of the hemocyte cell membrane and loss of vacuolar integrity, indicated by diffuse Lysotracker staining, were observed after 1 h of exposure to crypt contents. Similar results were obtained when the hemocytes were exposed to either 25% heat-treated crypt contents or 25% crypt contents in pH 7.5 Squid Ringer's buffer.

1. Kremer N, et al. (2014) The dual nature of haemocyanin in the establishment and persistence of the squid-vibrio symbiosis. *Proc Biol Sci* 281(1785):20140504.

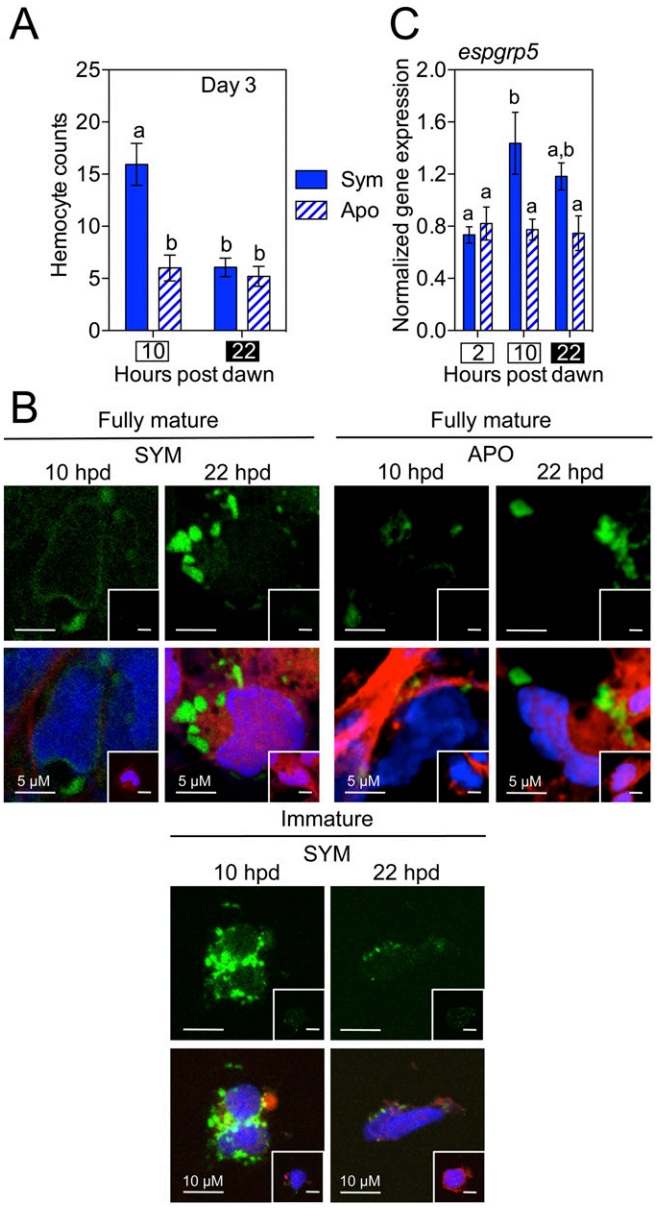

Fig. S2. Diel hemocyte-associated phenotypes. (*A*) Diel migratory behavior of hemocytes in symbiotic (Sym) or aposymbiotic (Apo) 3-d-old light organs, assessed during the day (white box) and night (black box). Data represent two independent experiments. "a" and "b" denote groups of statistically similar means, assessed by two-way ANOVA with post hoc Bonferroni *T*-tests. (*B*) Detection of *Es*Chit1-positive granules in hemocytes derived from symbiotic (SYM) and aposymbiotic (APO) squid 10 h and 22 h postdawn (hpd). *Insets* show the corresponding preimmune controls. (*Top*) Hemocytes were isolated from individual fully mature squid (>4 wk old). Observations were made from three independent samples. (*Bottom*) Detection of *Es*Chit1 in hemocytes isolated from pools of 15 immature squid (2 d posthatch). Images represent observations from two independent samples. (*C*) Transcription of the hemocyte-associated gene *espgrp5* (1) in 4-wk-old light organs measured during the day (white boxes), or at night (black box). Bars represent SEM, $n = 4$. a and b indicate groups of statistically similar means, assessed by two-way ANOVA with post hoc Bonferroni *T*-tests.

1. Collins AJ, Schleicher TR, Rader BA, Nyholm SV (2012) Understanding the role of host hemocytes in a squid/vibrio symbiosis using transcriptomics and proteomics. *Front Immunol* 3:91.

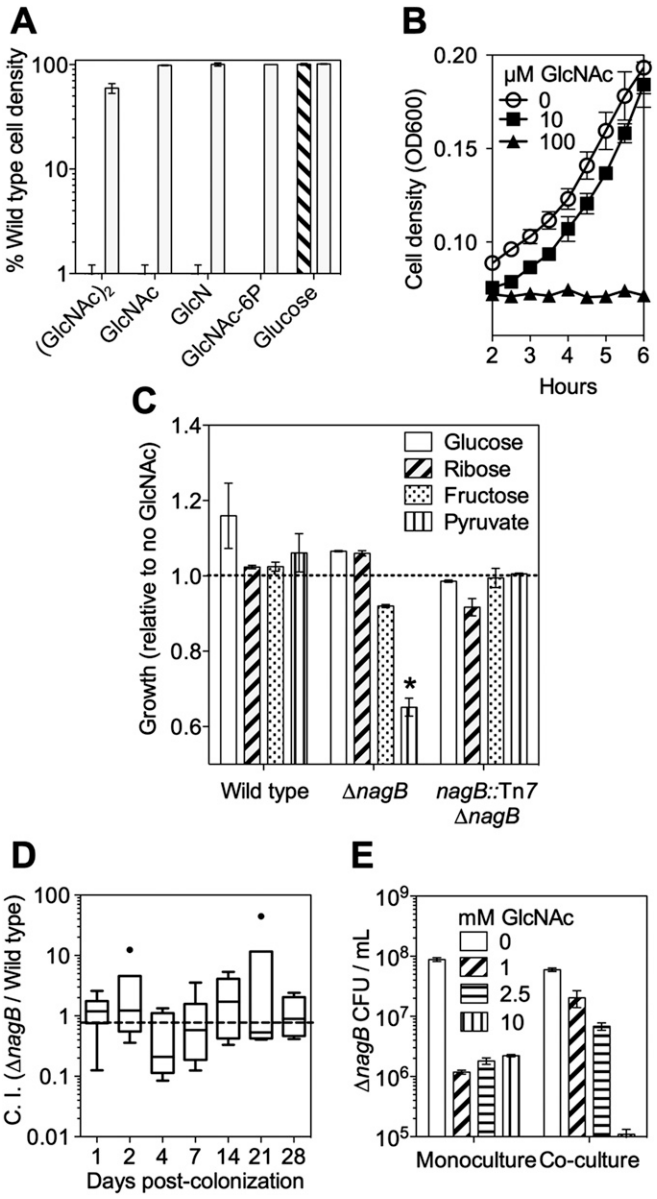

Fig. S3. Phenotypes of the COS biosensor strain, *ΔnagB*. (*A*) Growth of *ΔnagB* (hatched bar) and an *in cis* genetic complement, *ΔnagB* Tn*7*::*nagB* (open bars), relative to wild-type *V. fischeri* on different sugars. $(GlcNAc)_2$, chitobiose; GlcNAc, *N*-acetylglucosamine; GlcN, glucosamine. Bars indicate SEM, $n = 2$. (*B*) Concentration dependence of COS sensitivity. Cultures were grown in LBS with added GlcNAc, and growth was measured by optical density at 600 nm (OD_{600}). Bars indicate SEM, $n = 3$. (C) Ability of nongluconeogenic carbohydrates to reverse *ΔnagB* substrate inhibition. Growth of wild type, *ΔnagB*, and *ΔnagB* Tn*7*::*nagB* was assessed in the presence of both GlcNAc and the indicated, non-COS, carbohydrate. The capacity of the second carbohydrate to functionally complement substrate inhibition by GlcNAc was assessed by comparison with growth on the carbohydrate in the absence of GlcNAc. Bars indicate SEM, $n = 3$; * indicates a mean ratio of growth in the presence vs. absence of GlcNAc statistically different from 1.0, assessed by one-sample *T*-test. (*D*) Four-week co-colonization with both *ΔnagB* and wild-type *V. fischeri*. C.I., competitive index. Center bar indicates median C.I., inner fences are determined by Tukey's method, and outliers are shown as solid circles, $n = 6$ squid per time point. (*E*) Growth of *ΔnagB* with COS in complex medium. The *ΔnagB* strain was either cultured alone (monoculture) or cocultured with wild-type *V. fischeri* at an initial inoculum of 1:1. Bars indicate SEM, $n = 6$.

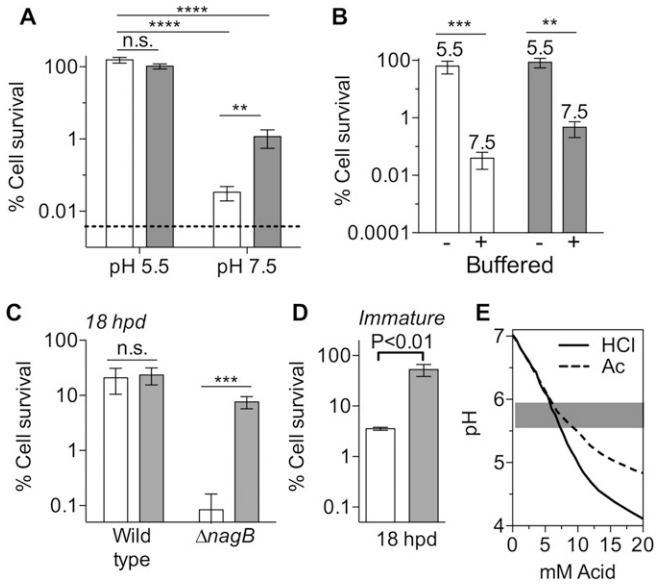

Fig. S4. Characterization of the conditions sufficient to induce the *V. fischeri* acid tolerance response and acidify the light-organ crypt. Throughout, bars indicate SEM, groups of statistically different means, determined by two-way ANOVA with post hoc Bonferroni *T*-tests. $*P < 0.05$, $**P < 0.01$, $***P < 0.005$, $****P < 0.001$; n.s., no significance. (*A–D*) Induction of acid tolerance was measured by calculating the survival of *V. fischeri* for 20 min in 0.1× organic acids medium (pH 4.75). *(A) V. fischeri* was grown either in pH 5.5 or in pH 7.5 media in the absence (open bars) or presence (solid bars) of 0.075× organic acids **(***n* = 4). (*B*) Induction of acid tolerance during growth of wild-type (open bars) or *ΔnagB* (solid bars) *V. fischeri* on 20 mM glucose in LBS medium. Medium was either buffered at pH 7.5 with 50 mM Pipes or left unbuffered. Final pH of the culture medium before killing challenge is noted above the bars (*n* = 4). (*C*) Symbiotic wild-type or *ΔnagB V. fischeri* were released from mature light organs at night (18 h postdawn, hpd). Released symbionts were assayed for their survival upon immediate acid exposure (open bars) or after preexposure to pH 5.5 medium containing 0.075× organic acids (solid bars) to compare the potential for induction of acid tolerance (*n* = 5). (*D*) Induction of acid tolerance of wild-type *V. fischeri* released from a pool of 20 2-d-old light organs at night (18 hpd) and assayed immediately for survival (open bar). A portion of the released cells was incubated for 1 h in 0.075× organic acids medium (pH 5.5) as a positive control for the capacity to induce acid tolerance (solid bar) (*n* = 2). *P* value was determined by two-tailed *T*-test. (*E*) Buffering capacity of cell-free squid hemolymph was determined by titration with either hydrochloric acid (HCl) or acetic acid (Ac). The pH range previously measured in light-organ crypts at night is indicated in the shaded area (1).

1. Kremer N, et al. (2014) The dual nature of haemocyanin in the establishment and persistence of the squid-vibrio symbiosis. *Proc Biol Sci* 281(1785):20140504.

>*E. scolopes* putative chitotriosidase EsChit1
MASTFATVFGVLSLCFLGLHLTNGEYKKVCYYTNWSQYRQIPAKFVPENISVSLCTHIIY
TFATLQNNHLKPFEWNDDSTPWMVGMYARVMKLKKKDPNLQVLLGVGGWNMGSYL
FSKMVANIQNRKMFYTNATGFLRKRNFDGLDIDWCYPGSRGSPAVDKKNYVSLLQETS
DYFLNESKISGKKRLLLTASIPVGKKTIIKGYDIPQVEKYLDFMNLMSYDYHGGSFDNVT
GHNSPLYPRKEETGDERTFNVNWSANYWVEHGVPRMKLNIGMPAYGRGFRLANHSCIL
PGCPSIGPNSPGQYTRLAGFLAYYEICDLIKKGAKVFRIADQKVPYLVYNNEWIGYDDV
KSLSIKVDWLKKNQFGGVAIWTLDLDDFFNGCGSGAYILIKTLTQELKLPSVEN

Fig. S5. Predicted protein sequence of the putative *Es*Chit1 chitotriosidase. Underlined sequence indicates peptide used for antibody production.

Table S1. Acetate excretion during aerobic growth on a single sugar

Strain	Sugar	mM acetate per OD unit	mM acetate produced per mM glucose used
Vibrio fischeri ES114	GlcNAc	9.8 ± 0.7	—
	Glucose	7.0 ± 0.2	0.9 ± 0.1
V. fischeri MJ11	GlcNAc	**11.9 ± 0.7**	—
	Glucose	**9.1 ± 0.5**	1.2 ± 0.1
Vibrio harveyi B392	GlcNAc	8.7 ± 0.2	—
	Glucose	6.7 ± 0.2	0.9 ± 0.1
Escherichia coli K12 (MG1655)	GlcNAc	**3.6 ± 0.1**	—
	Glucose	**4.0 ± 0.5**	**0.5 ± 0.1**

n = 3; ±, SEM; boldface type indicates a significantly different mean from ES114 on the same sugar. Strains were grown with shaking in minimal medium containing 5 mM GlcNAc (COS) or glucose; all strains grew to about the same yield (OD = 0.6–1.0). pH remained above 6.5 in all strains.

Table S2. Strains and plasmids used in this study

Strain or plasmid	Description	Source
V. fischeri		
ES114	Wild-type *E. scolopes* light-organ isolate	(1, 2)
MJ11	Wild-type isolate from fish, *Monocentris japonica*	(3)
TIM313	ES114 Tn*7*::pEVS107 Em^r	(4)
TIM302	ES114 *Tn7::gfp* Em^r	(4)
JAS101	ES114 Δ*nagB Tn7*::pEVS107 Em^r	(5)
JAS102	ES114 Δ*nagB Tn7*::pJAS102 Em^r	This study
V. harveyi		
B392	Wild-type isolate from seawater	(6)
E. coli		
DH5α-λpir	F^- φ80*lacZ*Δ*M15* Δ(*lacZYFargF*)U169 *supE44 deoR hsdR17 recA1 endA1 gyrA96 thi-1 relA1*, lysogenized with λ*pir*	(7)
K-12 (MG1655)	Wild-type *E. coli* $F^-\lambda$	ATCC47076
Plasmids		
pEVS104	R6Kori RP4 *oriT trb tra* Kn^r	(8)
pUX-BF13	R6Kori *tns bla*	(9)
pEVS107	R6Kori *oriT mini*-Tn*7 mob* Em^r Kn^r	(10)
pJAS102	*nagB::*Tn*7* pEVS107	This study

1. Boettcher KJ, Ruby EG (1990) Depressed light emission by symbiotic *Vibrio fischeri* of the sepiolid squid *Euprymna scolopes*. *J Bacteriol* 172(7):3701–3706.
2. Mandel MJ, Stabb EV, Ruby EG (2008) Comparative genomics-based investigation of resequencing targets in *Vibrio fischeri*: Focus on point miscalls and artefactual expansions. *BMC Genomics* 9:138.
3. Ruby EG, Nealson KH (1976) Symbiotic association of *Photobacterium fischeri* with the marine luminous fish *Monocentris japonica*; a model of symbiosis based on bacterial studies. *Biol Bull* 151(3):574–586.
4. Miyashiro T, Wollenberg MS, Cao X, Oehlert D, Ruby EG (2010) A single *qrr* gene is necessary and sufficient for LuxO-mediated regulation in *Vibrio fischeri*. *Mol Microbiol* 77(6): 1556–1567.
5. Miyashiro T, et al. (2011) The *N*-acetyl-D-glucosamine repressor NagC of *Vibrio fischeri* facilitates colonization of *Euprymna scolopes*. *Mol Microbiol* 82(4):894–903.
6. Reichelt JL, Baumann P (1973) Taxonomy of the marine, luminous bacteria. *Arch Mikrobiol* 94(4):283–330.
7. Hanahan D (1983) Studies on transformation of *Escherichia coli* with plasmids. *J Mol Biol* 166(4):557–580.
8. Stabb EV, Ruby EG (2002) RP4-based plasmids for conjugation between *Escherichia coli* and members of the Vibrionaceae. *Methods Enzymol* 358:413–426.
9. Bao Y, Lies DP, Fu H, Roberts GP (1991) An improved Tn7-based system for the single-copy insertion of cloned genes into chromosomes of gram-negative bacteria. *Gene* 109(1): 167–168.
10. McCann J, Stabb EV, Millikan DS, Ruby EG (2003) Population dynamics of *Vibrio fischeri* during infection of *Euprymna scolopes*. *Appl Environ Microbiol* 69(10):5928–5934.

Table S3. Primers used in this study

Gene	Primer sequences	Amplicon size, bp
Serine hydroxymethyl transferase	SerineHMT-qF: GTCCTGGTGACAAGAGTGCAATGA SerineHMT-qR: TTCCAGCAGAAAGGCACGATAGGT	148 (1)
40S Ribosomal protein S19	40S-qF: AATCTCGGCGTCCTTGAGAA 40S-qR: GCATCAATTGCACGACGAGT	103 (1)
Chitotriosidase 1	*Es*Chit1-qF: CCTGCATATGGACGAGGATTT *Es*Chit1-qR: GTATATTGACCAGGTGAGTTGGG	92
Peptidoglycan recognition protein 5	*Es*PGRP5-qF: TTGGAGCCCACACCAAGTTCTACA *Es*PGRP5-qR: CAAGACAGCAGGCGTTTCAATGCT	NR (2)

NR, not reported in original publication.

1. Wier AM, et al. (2010) Transcriptional patterns in both host and bacterium underlie a daily rhythm of anatomical and metabolic change in a beneficial symbiosis. *Proc Natl Acad Sci USA* 107(5):2259–2264.
2. Collins AJ, Schleicher TR, Rader BA, Nyholm SV (2012) Understanding the role of host hemocytes in a squid/vibrio symbiosis using transcriptomics and proteomics. *Front Immunol* 3:91.